

# Prediction of complex dielectric constants of polymer-clay nanocomposites

X. Yi<sup>a</sup>, H.L. Duan<sup>b</sup>, Y. Chen<sup>a</sup>, J. Wang<sup>a,\*</sup>

<sup>a</sup> *LTCS and Department of Mechanics and Engineering Science, College of Engineering, Peking University, Beijing 100871, PR China*

<sup>b</sup> *Institute of Nanotechnology, Forschungszentrum Karlsruhe, PO Box 3640, D-76021 Karlsruhe, Germany*

Received 26 April 2007; accepted 2 July 2007

Available online 18 July 2007

Communicated by J. Flouquet

## Abstract

In this Letter, simple theoretical models are presented to predict the influence of aspect ratio, orientation, distribution, and interphase of layered silicates on the dielectric properties of polymer-clay nanocomposites. The predictions are in good agreement with experimental data. The results show that the morphology of the clay fillers and the thickness and dielectric properties of the interphases play an important role in determining the dielectric properties of polymer-clay nanocomposites.

© 2007 Elsevier B.V. All rights reserved.

*Keywords:* Polymer-clay nanocomposites; Dielectric properties; Interphase; Morphology

## 1. Introduction

Polymer-clay nanocomposites (PCNs) are an important set of organic–inorganic hybrid materials with good thermal stability, outstanding barrier properties and high specific stiffness [1–6]. The dielectric properties of PCNs, especially, those with low dielectric constants and dielectric losses [7,8], have attracted a lot of attention because of their significant applications in integrated circuits, microelectronics and insulating devices and membrane technology [9]. Polymer matrices of PCNs include polymethyl methacrylate (PMMA) and polyimide (PI), etc. Clay fillers such as montmorillonite, saponite, kaolinite, mica and hectorite are crystalline materials which are composed of plate-shaped crystals about 1 nm thick with diameter from 50 to 1500 nm. As the most commonly used clay for the production of PCNs, montmorillonite (MMT) belongs to the family of 2:1 phyllosilicates. Its crystal lattice consists of sandwich structure layers made of two tetrahedral coordinated silicon atoms fused to an edge-shared octahedral sheet of either aluminum or magnesium hydroxide. Mica also processes a 2:1 structure, similar

to MMT, but compared with MMT, mica is difficult to be exfoliated by polymer molecules.

To the authors' knowledge, currently, there are no theoretical models in the literature to predict the effective dielectric properties of PCNs taking into account the aspect ratio, orientation, morphology and the spatial distribution of the clay fillers, and the effect of the interphases. In this Letter, we present simple models and a microstructural scheme to systematically predict the effective dielectric properties of PCNs while taking into account these microstructural details. It is shown that the predictions are in very good agreement with the experimental data.

## 2. Model and formalism

In general, there are three typical dispersions of layered silicates in polymer matrices: exfoliated dispersion where layered silicates are separated into individual layers (platelets) [Fig. 1(a)]; intercalated dispersion where polymer chains are inserted into the space between the layers of silicates resulting in well-ordered, laminated nanostructures [Fig. 1(c)]; phase-separated dispersion where layered silicates exist in original aggregated state with different sizes, and the polymer and clay fillers remain immiscible [Fig. 1(e)] [10]. Besides these three representative morphologies, there are also blends of exfoliated/intercalated [Fig. 1(b)] and intercalated/phase-separated

\* Corresponding author.

E-mail address: [jxwang@pku.edu.cn](mailto:jxwang@pku.edu.cn) (J. Wang).

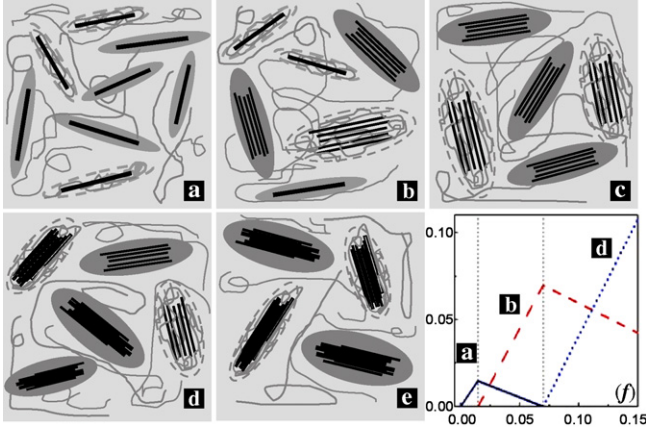


Fig. 1. Diagram of clay morphologies of PCNs: (a) fully exfoliated; (b) partially exfoliated and partially intercalated; (c) severely intercalated; (d) partially intercalated and partially aggregated; (e) severely aggregated. The dark grey zones are interphases; (f) shows the change of the dispersions as the clay content increases (from 0 to 15 vol%). Solid, dash and dot lines represent the volume fractions of exfoliated, intercalated and phased-separated silicates, respectively.

ones [Fig. 1(d)]. As the MMT content increases, the morphology may change gradually from exfoliated and intercalated (about 3–5 wt%) dispersions to partially intercalated and aggregated ones (10 wt% and more) [11]. Because mica is difficult to be intercalated and exfoliated, for PI-mica nanocomposites there may be just aggregated silicates with different sizes [Fig. 1(e)]. The orientation and mobility of polymer molecules adjacent to the surface of clay fillers are affected and their movements may be constrained. This gives rise to an interphase whose physical properties are different from these of the polymer matrix [2,5].

In predicting the effective dielectric constants of the PCNs, the three typical particles in Figs. 1(a), (c) and (e) together with their surrounding interphases are simulated as equivalent spheroidal homogeneous particles, and then these equivalent homogeneous particles are embedded in the respective matrices. Therefore, the predictions of the effective dielectric constants of the composites consist of two hierarchical steps. The first step is to calculate the effective dielectric constants of the equivalent particles, and the second is to predict those of the composites containing the equivalent particles and the matrices. For exfoliated and phase-separated dispersions [Figs. 1(a), (e)], the dielectric constants  $\varepsilon_c$  of the individual platelets and aggregated clay fillers, which are surrounded by the interphases, are the same as the dry clay. The intercalated particles in Fig. 1(c) can be treated as well-ordered laminates surrounded by the interphase. We use parallel and series rules-of-mixtures to evaluate the complex dielectric constants of these laminates, and they are  $\varepsilon_{l\parallel} = \varepsilon_c v_c^* + \varepsilon_p(1 - v_c^*)$  and  $\varepsilon_{l\perp} = 1/(v_c^*/\varepsilon_c + (1 - v_c^*)/\varepsilon_p)$ , where subscript  $l$  indicates the quantities related to the laminates, and subscripts  $\parallel$  and  $\perp$  refer to the quantities parallel and perpendicular to the layer plane, respectively.  $v_c^*$  is the volume fraction of the parallel layers in the laminates, and  $\varepsilon_p$  is the complex dielectric constant of the polymer chains in the galleries of the parallel layers, which is different from the dielectric constant  $\varepsilon_l$  of the interphase and the dielectric constant  $\varepsilon_m$  of

the matrix. In this Letter,  $\varepsilon = \varepsilon' - i\varepsilon''$  denotes the complex dielectric constants. Then, the effective dielectric constants of the equivalent particles in Figs. 1(a), (c) and (e) are given by [12]

$$\frac{\varepsilon_i^e}{\varepsilon_l} = 1 + \frac{f_r^*(\varepsilon_i^r - \varepsilon_l)}{\varepsilon_l + L_i^r(\varepsilon_i^r - \varepsilon_l)(1 - f_r^*)} \quad (i = \parallel, \perp), \quad (1)$$

where

$$L_{\parallel}^r = \frac{1}{2(\chi_r^2 - 1)} \left( \frac{\chi_r^2 \arctan \sqrt{\chi_r^2 - 1}}{\sqrt{\chi_r^2 - 1}} - 1 \right),$$

$$L_{\perp}^r = 1 - 2L_{\parallel}^r \quad (2)$$

and  $f_r^*$  represents the volume fraction of the clay (platelet, Fig. 1(a); laminate, Fig. 1(c); aggregate, Fig. 1(e)) in the equivalent spheroidal particles.  $\chi_r$  is the usual aspect ratio of the spheroidal equivalent particles.  $\chi_r > 1$  for oblate spheroids, and  $\chi_r < 1$  for prolate spheroids (e.g., [13]). For spherical inclusions,  $L_{\parallel}^r = L_{\perp}^r = 1/3$ . For clay platelets and aggregated clay fillers [Figs. 1(a), (e)],  $\varepsilon_i^r$  should be replaced by  $\varepsilon_c$ ; for laminated particles [Fig. 1(c)] whose complex dielectric constants are transversely isotropic,  $\varepsilon_i^r$  in Eq. (1) should be replaced by  $\varepsilon_{l\parallel}$  and  $\varepsilon_{l\perp}$ .

After obtaining the dielectric properties of the equivalent particles, next, we calculate the effective dielectric constants of the PCNs containing aligned clay fillers with a spheroidal spatial distribution [13]. These composites exhibit transverse isotropy. The dielectric constant  $\varepsilon_{\parallel}$  in the direction of the isotropic plane and the component  $\varepsilon_{\perp}$  perpendicular to it are [13]

$$\frac{\varepsilon_i}{\varepsilon_m} = 1 + \left[ \left( \sum_{e=1}^N G_i^e \right)^{-1} - L_i^V \right]^{-1} \quad (i = \parallel, \perp), \quad (3)$$

where  $N$  denotes the types of discrete equivalent composite particles, and  $L_{\parallel}^V$  and  $L_{\perp}^V$  are the depolarization factors of the distribution ellipsoid expressed in Eq. (2) while  $\chi_r$  is replaced by the aspect ratio of the distribution ellipsoid [13].  $G_i^e$  is given by

$$G_i^e = f_e \frac{\varepsilon_i^e - \varepsilon_m}{\varepsilon_m + L_i^e(\varepsilon_i^e - \varepsilon_m)} \quad (i = \parallel, \perp), \quad (4)$$

where  $\varepsilon_i^e$  depends on different dispersions in Fig. 1 and is given in Eq. (1).  $f_e$  is the volume fraction of the equivalent composite particles. For PCNs containing randomly oriented and distributed clay fillers, the isotropic effective complex dielectric constant is given by [13]

$$\frac{\varepsilon}{\varepsilon_m} = 1 + \left[ \left( \sum_{e=1}^N \frac{2G_{\parallel}^e + G_{\perp}^e}{3} \right)^{-1} - \frac{1}{3} \right]^{-1}, \quad (5)$$

where  $G_{\parallel}^e$  and  $G_{\perp}^e$  are given in Eq. (4).

Incorporation of a low content of clay fillers can efficiently decrease the dielectric constants of PCNs. However, as the clay content increases to a certain critical volume fraction, this decreasing effect declines [7,8]. Considering the change of the morphology of layered silicates, we present a microstructural scheme to characterize this phenomenon. For clay minerals such as MMT which are easy to be exfoliated, we introduce two

parameters to simulate the change of the morphology: a saturation ratio of exfoliation,  $f_{ef}$ , and a saturation ratio of intercalation,  $f_{it}$ . If the volume fraction  $f$  of clay fillers is less than  $f_{ef}$ , they exist as individual platelets [Fig. 1(a)]. When  $f = f_{ef}$ , the saturation of exfoliation is reached. Assuming that the individual platelets are evenly dispersed in the matrix, so the composite can be divided into many equal regions and each contains an individual platelet. With the further increase of clay content ( $f > f_{ef}$ ), the added clay fillers (volume fraction  $f - f_{ef}$ ) cannot fully react with the polymer molecules, so they may form intercalated structures together with some exfoliated ones, which results in the decrease of the content of the exfoliated platelets [Fig. 1(b)]. Here, we introduce a parameter  $\eta$  to represent the number of platelets in an individual intercalated structure, so the morphology change during the above process can be expressed by the following equation:

$$f_c^{ef} = \begin{cases} f & \text{if } f \leq f_{ef}, \\ f - \frac{\eta(f - f_{ef})}{(1 - f_{ef})(\eta - 1)} & \text{if } f > f_{ef}, \end{cases} \quad (6)$$

where  $\eta > 1$ , and  $f_c^{ef}$  is the volume fraction of the exfoliated clay fillers. The volume fraction of the intercalated clay fillers is  $f_c^{it} = f - f_c^{ef}$ . It is pointed out that Feng [14], in predicting the effective elastic moduli of polymer-clay nanocomposites, proposed a formula to delineate the change of the morphology of the silicates. When  $\eta \rightarrow \infty$ , Eq. (6) reduces to that of Feng [14].

When exfoliated clay fillers vanish [Fig. 1(c)], namely, when  $f_c^{ef} = 0$ , we define the volume fraction of clay fillers  $f$  as the saturation ratio of intercalation  $f_{it}$ , and  $f_{it} = \eta f_{ef} / [1 + (\eta - 1)f_{ef}]$ . When  $f_{ef} < f < f_{it}$ , there is a blend of exfoliated and intercalated layered silicates [Fig. 1(b)]. If  $f > f_{it}$ , intercalated and phase-separated clay fillers coexist [Fig. 1(d)], and in this case Eq. (6) can be extended to depict the morphological change from intercalation to phase-separation, and in this case,  $\eta$  represents the ratio of the number of platelets in an aggregated particle to that in an individual intercalated structure.

For clay particles which are difficult to be intercalated or exfoliated such as mica [6,8], we assume that there exists a saturation ratio of phase-separation,  $f_{ag}$ , when  $f \leq f_{ag}$ , mica particles exist as aggregated particles with small size and if  $f > f_{ag}$ , there is a blend of small and large aggregated clay particles [Fig. 1(e)]. In this case,  $f = f_{ef}$  in Eq. (6) should be replaced by  $f = f_{ag}$  and  $\eta$  represents the ratio of the number of platelets in a large aggregated particle to that in a small one. Eqs. (3) and (5) can be used along with the effect of morphological change to predict the effective properties.

### 3. Numerical results and discussion

The relative dielectric constants  $\varepsilon'$  versus the volume fractions of randomly distributed MMT ( $\varepsilon_c = 5.5 - 0.00165i$ ) and mica ( $\varepsilon_c = 5 - 0.0015i$ ) fillers in PI matrix ( $\varepsilon_I = 3.36 - 0.03i$ ) are shown in Fig. 2 [7,8,15]. In the region AB, the MMT fillers exist as fully exfoliated platelets and are evenly dispersed in the matrix, and at the point B, the saturation of exfoliation is reached. From the point B to C, the MMT morphology changes from full exfoliation to intercalation gradually, and at

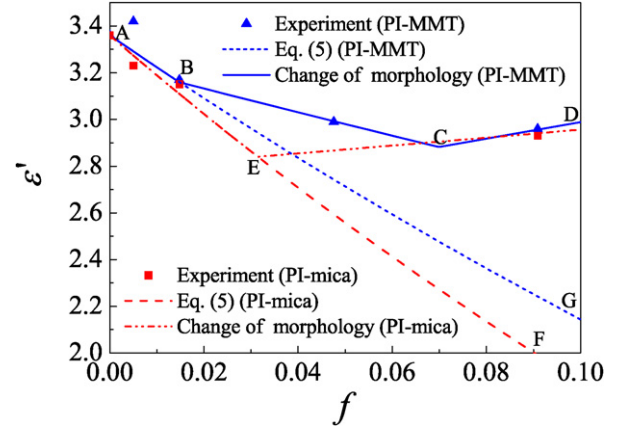


Fig. 2. Comparison of the experimental data [7,8] of the effective dielectric constants of PI-MMT and PI-mica hybrid films at 1 kHz, 150 °C with theoretical predictions. The straight lines AF and AG are the predictions without considering the change of morphology.

the point C the intercalation saturation is reached. The region CD depicts the gradually morphological change of the MMT fillers from intercalation to phase-separation. Similar to the case of PI-MMT, mica fillers exist as small aggregated particles in the region AE, and the saturation of phase-separation is reached at the point E. In the region ED, the mixture of small and large aggregated mica particles prevails. The parameters used in Fig. 2 are as follows. The MMT and mica layers are about 220 nm and 1300 nm in length, respectively, with a thickness 1 nm. For PI-MMT nanocomposites, the interlayer spacing of intercalated MMT is 1.34 nm [7]. We assume that the thickness of the interphase  $t = 5$  nm,  $f_{ef} = 1.48\%$  (3 wt%),  $\varepsilon_p = 1.68 - 0.015i$ ,  $\varepsilon_I = 2.15 - 0.019i$ . The intercalated silicate stacks consist of 5 layers ( $\chi_r \approx 34.8$ ), and the aggregated clay consist of 25 layers ( $\chi_r \approx 8.8$ ). Then  $\varepsilon_{I\parallel} = 0.24\varepsilon_p + 0.76\varepsilon_c$  and  $\varepsilon_{I\perp} = 1/(0.24/\varepsilon_p + 0.76/\varepsilon_c)$ . With all these data, the theoretical predictions are in good agreement with the experimental data reported in the literature. For PI-mica films, we assume that  $t = 20$  nm,  $f_{ag} = 3.15\%$  (6.5 wt%),  $\varepsilon_I = 1.68 - 0.015i$ . When  $f \leq f_{ag}$ , the small aggregated mica fillers are assumed to be composed of 5 layers ( $\chi_r \approx 325$ ), and when  $f > f_{ag}$ , the large aggregated mica fillers are composed of 100 layers ( $\chi_r \approx 13$ ). The theoretical results also agree well with the experimental data. The straight lines AF and AG in Fig. 2 show that the predictions without considering the change of the morphology deviate from the experimental data as the clay contents increase.

In order to investigate the effect of the interphase, in Fig. 3, we compare the effective dielectric constants of three ideal types of PCNs, namely, exfoliated, phase-separated and intercalated, for PI-MMT nanocomposites with different properties of the interphase. Here, for expediency, we assume that the dielectric constants of the polymer in the galleries and the interphase are  $\varepsilon_p = \varepsilon_I = \xi\varepsilon_m$ . The other material parameters used are the same as those in Fig. 2. Fig. 3 shows that the clay fillers should be fully exfoliated into individual platelets to maximize their effect, and the dielectric properties of the interphases dominate the effective complex dielectric constants of PCNs.

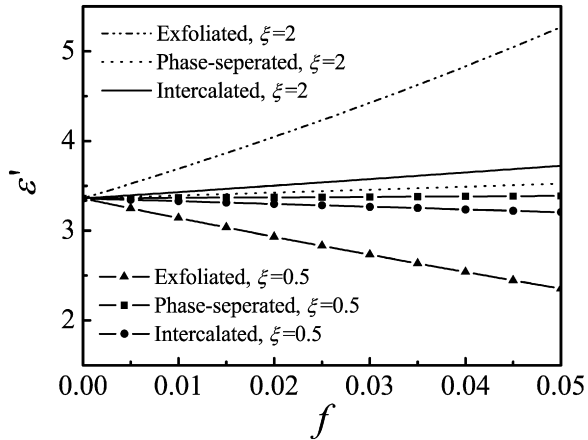


Fig. 3. Comparison of effective dielectric constants of three idealized types of PI-MMT nanocomposites.

For PCNs with parallel clay fillers, the complex dielectric constants  $\varepsilon_{\perp}$  and  $\varepsilon_{\parallel}$  exhibit characteristics similar to those  $\varepsilon'$  in Fig. 3.

#### 4. Conclusions

In this Letter, we present micromechanical models and a microstructural scheme to predict the complex dielectric constants of PCNs containing clay fillers of various shapes and spatial distributions. The effects of the morphology and the interphase on the effective complex dielectric constants are highlighted. It is shown that the incorporation of an interphase is particularly important for the prediction of the effective properties. The predicted effective complex dielectric constants of PCNs

with different clay contents agree well with the experimental data reported in the literature.

#### Acknowledgements

Yi, Chen and Wang acknowledge the support of the National Natural Science Foundation of China under Grant No. 10525209. Duan acknowledges the support of the Alexander von Humboldt Research Fellowship.

#### References

- [1] P. Calvert, *Nature* 383 (1996) 300.
- [2] Y. Kojima, A. Usuki, M. Kawasumi, A. Okada, Y. Fukushima, T. Kurauchi, O. Kamigaito, *J. Mater. Res.* 8 (1993) 1185.
- [3] C. Lu, Y.M. Mai, *Phys. Rev. Lett.* 95 (2005) 088303.
- [4] J. Wang, R. Pyrz, *Compos. Sci. Technol.* 64 (2004) 925.
- [5] J. Wang, R. Pyrz, *Compos. Sci. Technol.* 64 (2004) 935.
- [6] L.A. Utracki, *Clay-containing Polymeric Nanocomposites*, Rapra, Shawbury, 2004.
- [7] Y.H. Zhang, Z.M. Dang, S.Y. Fu, J.H. Xin, J.G. Deng, J. Wu, S. Yang, L.F. Li, Q. Yan, *Chem. Phys. Lett.* 401 (2005) 553.
- [8] Y.H. Zhang, Z.M. Dang, J.H. Xin, W.A. Daoud, J.H. Ji, Y. Liu, B. Fei, Y. Li, J. Wu, S. Yang, L.F. Li, *Macromol. Rapid Commun.* 26 (2005) 1473.
- [9] H. Treichel, G. Ruhl, P. Ansmann, R. Würfl, Ch. Müller, M. Dietmeier, *Microelectron. Eng.* 40 (1998) 1.
- [10] T. Lan, T.J. Pinnavaia, *Chem. Mater.* 6 (1994) 2216.
- [11] Y.H. Zhang, J.T. Wu, S.Y. Fu, S.Y. Yang, Y. Li, L. Fan, R.K.Y. Li, L.F. Li, Q. Yan, *Polymer* 45 (2004) 7579.
- [12] C.W. Nan, K.F. Cai, R.Z. Yuan, *Ceramics Int.* 22 (1996) 457.
- [13] H.L. Duan, B.L. Karihaloo, J. Wang, X. Yi, *Phys. Rev. B* 73 (2006) 174203.
- [14] X.Q. Feng, *Chin. Sci. Bull.* 46 (2001) 348 (in Chinese).
- [15] D.A. Robinson, *Vadose Zone J.* 3 (2004) 705.